



2012

# Improved quantum efficiency in InGaN light emitting diodes with multi-double-heterostructure active regions

X. Li

*Virginia Commonwealth University*

Serdal Okur

*Virginia Commonwealth University, okurs@vcu.edu*

F. Zhang

*Virginia Commonwealth University*

*See next page for additional authors*

Follow this and additional works at: [http://scholarscompass.vcu.edu/egre\\_pubs](http://scholarscompass.vcu.edu/egre_pubs)

 Part of the [Electrical and Computer Engineering Commons](#)

Li, X., Okur, S., Zhang, F., et al. Improved quantum efficiency in InGaN light emitting diodes with multi-double-heterostructure active regions. *Applied Physics Letters*, 101, 041115 (2012). Copyright © 2012 AIP Publishing LLC.

Downloaded from

[http://scholarscompass.vcu.edu/egre\\_pubs/37](http://scholarscompass.vcu.edu/egre_pubs/37)

This Article is brought to you for free and open access by the Dept. of Electrical and Computer Engineering at VCU Scholars Compass. It has been accepted for inclusion in Electrical and Computer Engineering Publications by an authorized administrator of VCU Scholars Compass. For more information, please contact [libcompass@vcu.edu](mailto:libcompass@vcu.edu).

---

**Authors**

X. Li, Serdal Okur, F. Zhang, S. A. Hafız, Vitaliy Avrutin, Umit Ozgur, Hadis Morkoç, and K. Jarašiūnas

## Improved quantum efficiency in InGaN light emitting diodes with multi-double-heterostructure active regions

X. Li,<sup>1</sup> S. Okur,<sup>1</sup> F. Zhang,<sup>1</sup> S. A. Hafiz,<sup>1</sup> V. Avrutin, Ü. Özgür,<sup>1,a)</sup> H. Morkoç,<sup>1</sup> and K. Jarašiūnas<sup>2</sup>

<sup>1</sup>Department of Electrical and Computer Engineering, Virginia Commonwealth University, Richmond, Virginia 23284, USA

<sup>2</sup>Semiconductor Optoelectronics Department, Institute of Applied Research, Vilnius University, Vilnius, Lithuania

(Received 11 June 2012; accepted 12 July 2012; published online 25 July 2012)

InGaN light emitting diodes (LEDs) with multiple thin double-heterostructure (DH) active regions separated by thin and low energy barriers were investigated to shed light on processes affecting the quantum efficiency and means to improve it. With increasing number of 3 nm-thick DH active layers up to four, the electroluminescence efficiency scaled nearly linearly with the active region thickness owing to reduced carrier overflow with increasing total thickness, showing almost no discernible efficiency degradation at high injection levels up to the measured current density of 500 A/cm<sup>2</sup>. Comparison of the resonant excitation dependent photoluminescence measurements at 10 K and room temperature also confirmed that further increasing the number of DH layers beyond six results in degradation of the material quality, and therefore, increasing nonradiative recombination. Using multiple DH active regions is shown to be a superior approach for quantum efficiency enhancement compared with simply increasing the single DH thickness or the number of quantum wells in LED structures due to better material quality and larger number of states available. © 2012 American Institute of Physics. [<http://dx.doi.org/10.1063/1.4739419>]

As InGaN based light-emitting diode (LED) technology continues to develop and mature, high brightness LEDs retaining high quantum efficiencies at high injection levels (>100 A/cm<sup>2</sup>) have become even more desirable to replace the prevailing incandescent lamps and fluorescent tubes in general lighting.<sup>1</sup> However, the quantum efficiency of typical InGaN multi quantum well (MQW) LEDs peaks at current densities even as low as ~10 A/cm<sup>2</sup> and drops with increasing injection by a factor of as much as 2 in some reported cases. Although debates still persist on the origins of “efficiency droop,” carrier overflow has been reported to be the substantial component.<sup>2–4</sup> In order to avoid carrier overflow and increase the light output, LEDs must employ thick double heterostructure (DH) or MQW active regions.

In InGaN MQWs normally adopting thick (>10 nm) GaN barriers light is emitted mainly from the topmost QWs adjacent to *p*-GaN due to the poor hole transport.<sup>5,6</sup> DH active regions on the other hand can ensure more uniform hole spreading across the active region due to the absence of barriers and consequently have paved the way for negligible drop in quantum efficiencies beyond current densities of ~150 A/cm<sup>2</sup>.<sup>7</sup> Moreover, DH LEDs possess bulk-like 3D density of states (DOS), and therefore, can accommodate more carriers than thin QWs having constant 2D DOS. However, among the ramifications of DHs are the degradation of InGaN structural quality with increasing thickness and separation of electron and hole wavefunctions due to the polarization field in the *c*-plane variety.<sup>8,9</sup> Therefore, keeping the DH layer thin (3 nm) but stacking multiple of them separated by thin and low barriers (for ameliorating hole transport<sup>10</sup>) in the active regions could be a promising approach to maintain

high material quality and overcome the efficiency loss at high driving currents. In this work, we demonstrate that by using 3 nm-thick multi-DH active layers separated by 3 nm-thick low-energy In<sub>0.06</sub>Ga<sub>0.94</sub>N barriers the electroluminescence (EL) is enhanced dramatically, in proportion with the number of DH layers up to 4 without discernible efficiency loss at high injection levels. Moreover, under resonant optical excitation, emission intensities at 10 K increase linearly with excitation power, indicating nearly unity quantum efficiency, and scale with the effective active region thickness for a given excitation density. This study markedly differs from the prior work<sup>9</sup> in that with increasing number of active region DH layers carrier overflow is unequivocally shown to reduce significantly, and material degradation beyond 6 DH layers is found to be the efficiency limiting factor for a given electron injector design. We also show that using multi-DH active regions is a more effective way to achieve high LED efficiency compared with solely increasing single DH thickness or using a MQW active region.

The *c*-plane multi-DH InGaN LED structures, emitting at ~425 nm, were grown on ~5 μm-thick *n*-type GaN templates on sapphire substrates in a vertical low-pressure metalorganic chemical vapor deposition (MOCVD) system. The GaN templates employed an *in situ* SiN<sub>x</sub> nanonetwork to reduce the dislocation density down to mid-10<sup>8</sup> cm<sup>-3</sup>.<sup>11</sup> The active regions contained one to eight 3 nm-thick In<sub>0.15</sub>Ga<sub>0.85</sub>N DH active layers separated by 3 nm In<sub>0.06</sub>Ga<sub>0.94</sub>N barriers. All the structures incorporate a staircase electron injector (SEI) for efficient thermalization of hot electrons prior to injection into the active region,<sup>3</sup> and a 60-nm Si-doped (2 × 10<sup>18</sup> cm<sup>-3</sup>) In<sub>0.01</sub>Ga<sub>0.99</sub>N underlying layer for improving the quality of overgrown layers. The SEI consists of two 5 nm InGaN layers with step-increased In compositions of 4% and 8%, inserted

<sup>a)</sup>Email: uozgur@vcu.edu.

in the given order below the active region. The LED structures were completed with 100 nm-thick Mg-doped *p*-GaN layers having  $6 \times 10^{17} \text{ cm}^{-3}$  hole density, as determined by Hall measurements on a separate calibration sample. Device fabrication procedures using standard photolithography are described elsewhere.<sup>9</sup> The EL efficiencies were compared with those of LED structures with either 9 nm thick  $\text{In}_{0.15}\text{Ga}_{0.85}\text{N}$  DH or six period MQW [ $\text{In}_{0.15}\text{Ga}_{0.85}\text{N}$  (2 nm)/ $\text{In}_{0.06}\text{Ga}_{0.94}\text{N}$  (3 nm)] active regions.

A common procedure to evaluate the internal quantum efficiency (IQE) involves excitation-dependent photoluminescence (PL) measurements and comparison of the PL intensities at low and room temperatures by assuming 100% IQE at low temperature.<sup>12,13</sup> Excitation power dependent resonant PL measurements were performed at both 10 K and 295 K using 385 nm excitation from a frequency doubled Ti:sapphire laser ensuring photo-generation of carriers only in the LED active regions. The highest excitation density used corresponds to an average carrier concentration of  $\sim 10^{18} \text{ cm}^{-3}$  in the single DH LED structure. As the collected PL intensity is proportional to excitation intensity,  $L_{PL} \propto I_{exc}^m$ , the linear dependence ( $m \approx 1$ ) for all structures at 10 K [see Fig. 1(a)] indicate that the radiative recombination dominates, i.e.,  $\tau_{Rad} \ll \tau_{nonRad}$ , where  $\tau_{Rad}$  and  $\tau_{nonRad}$  are the radiative and nonradiative lifetimes, respectively. It is, therefore, reasonable to assume that the quantum efficiencies are nearly one at 10 K for all DH LEDs, omitting the negligibly slight deviations. The room temperature data [Fig. 1(b)], however, show superlinear dependence ( $m \approx 1.4$ -1.95) for low excitations, which is attributed to the notable impact of nonradiative recombination ( $m=2$  in case of constant  $\tau_{nonRad}$ ). As the excitation density is increased, the slope gradually approaches to  $m=1$  ( $I_{PL} \propto I_{exc}$ ). The gradually decreasing slope in the intermediate excitation regime indicates strong competition between nonradiative and radiative processes and can be attributed to decreasing radiative lifetime, beneficial, for moderate injections. Another process to be kept in mind is that with further increase of excitation, saturation of localized states and delocalization of carriers (particularly holes, as the electron density in the wells is in mid- $10^{17} \text{ cm}^{-3}$ ) may allow access to additional nonradiative centers and result in enhanced recombination rate with respect to low excitation.<sup>14,15</sup> Moreover, Coulomb screening of the quantum confined Stark effect (QCSE) with increasing excitation leads to an increased interband recombination rate  $1/\tau_{Rad}(N) \propto BN$ , where  $B$  is the bimolecular recombination

coefficient and  $N$  is injected carrier density. The IQE values deduced from ratio of PL intensities at 300 K and 10 K at the highest excitation density employed are shown in the inset of Fig. 1(b). The quad 3 nm DH LED exhibits an IQE, so determined, of  $\sim 46\%$  whereas increasing the number of 3 nm DH active regions to 6 and 8 lowers the IQE to 36% and 16%, respectively, indicative of active region degradation with increasing overall thickness due to plausibly strain relaxation and increased interface roughness. This degradation is evident also from the room temperature PL efficiencies, defined as the collected integrated PL intensity normalized to the incident laser power, shown in Fig. 1(c). Notably, the PL efficiencies nearly scale with the number of DH layers up to 6 due to increased absorption and emitting volume, showing  $\sim 2$ , 4, and 6.5 fold increase for dual, quad, and hexa DHs compared to single DH at an excitation density of  $1.5 \text{ kW/cm}^2$ , but no further improvement for the octa DH LED which is most likely a manifestation of material degradation.

To study the impact of carrier overflow and other carrier transport features, we measured EL efficiencies on-wafer (unpackaged) with light output collected primarily normal to the sample surface by an optical fiber. The integrated EL intensities vs. injection current are shown in Fig. 2. The integrated EL intensity,  $L_{EL}$ , can be described by a power dependence on the injection current density as  $L_{EL} \propto J^m$ , where the power index  $m$ , as in the case of optical excitation, reflects an effective rate of recombination processes within a given range of current densities.<sup>16</sup> The superlinear growth of EL intensity ( $m \sim 1.4$  for single,  $\sim 1.3$  for dual and quad, and  $\sim 1.6$  for hexa and octa DH LEDs) at low current densities is again attributed to nonradiative recombination. Smaller  $m$  values suggest lower density of nonradiative recombination centers in single, dual, and quad DH LEDs compared to hexa and octa DH LEDs. The EL intensity changes nearly linearly at high current levels; therefore, EL efficiency tends to be constant [Fig. 2 inset].

As presented in the inset of Fig. 2, the EL efficiency for the multi-double-heterostructure with up to 4 DH layers increases rapidly with current injection and reaches its maximum at  $\sim 35$ – $40 \text{ A/cm}^2$ . Compared to the single 3 nm DH LED, the peak EL efficiencies for dual and quad DH LEDs are higher by 1.6 and 3.5 times, respectively. Unlike in the case of optical injection, this significant improvement on EL efficiency cannot simply be explained by increased emitting volume as for a given current density overall carrier concentration is the same. Therefore, the data unequivocally

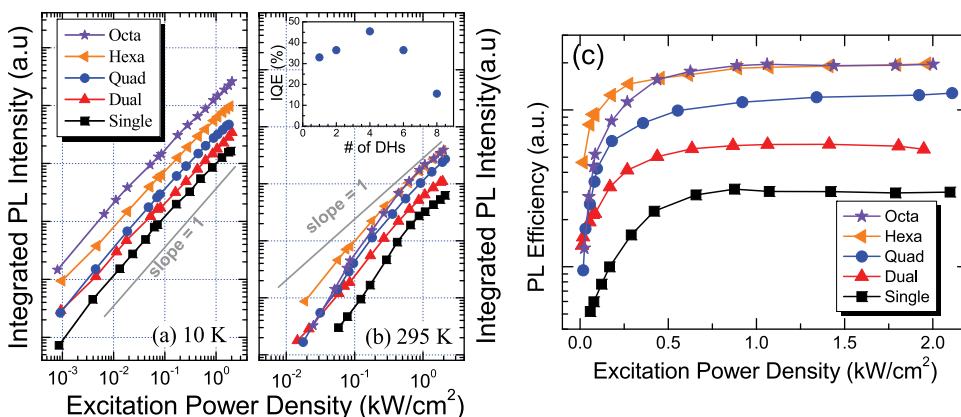


FIG. 1. Integrated PL intensity as a function of excitation power density at (a) 10 K and (b) 295 K; gray solid lines indicate slope of 1 and the inset of (b) displays the PL-IQE vs. the number of 3 nm DHs in the active region; (c) PL efficiencies of multi-3 nm DHs vs. excitation power density at room temperature.

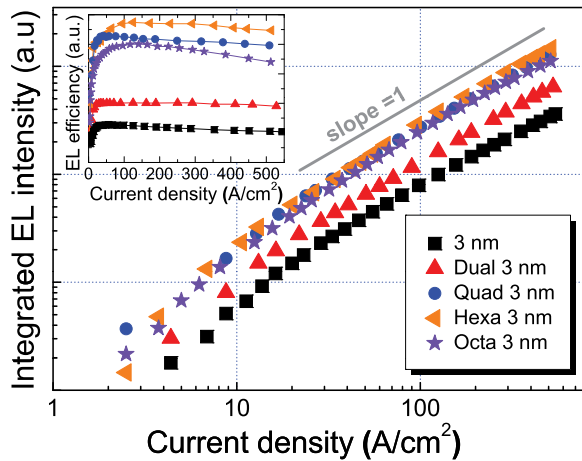


FIG. 2. The integrated EL intensity dependence on current density (the grey-solid line indicates slope of 1); the inset shows EL efficiencies of multi-3 nm DHs vs. injected carrier density.

indicate that increasing the number of 3 nm DH layers (from 1 to 6) decreases the overflow of injected carriers considerably (i.e., more of the injected carriers are captured by the active region), while further increase in number of DH layers (8) aggravates by introducing more nonradiative recombination centers due to degradation of the active region quality.

It is important to note that although the 5 nm+5 nm SEI (electron cooler) design used here has been shown to be an effective replacement for the  $\text{Al}_{0.15}\text{Ga}_{0.85}\text{N}$  electron blocking layer for reducing electron overflow in structures with multiple QWs and wider DHs (6 and 9 nm),<sup>17</sup> it must be optimized for a given active layer to fully prevent electron overflow. Based on the hot electron model reported in Ref. 17, the percentage ( $p$ ) of electrons captured by and recombine in the active region is increased to 76% in quad DH LED compared to 48% and 60% for single and dual 3 nm DH LEDs, respectively, at a current density of  $\sim 500 \text{ A/cm}^2$ .

The above somewhat crude estimates are simply based on single active regions with effective thicknesses equal to the number of DH active layers multiplied by 3 nm, i.e., 3, 6, and 12 nm for single, dual, and quad 3 nm DH, respectively. Our preliminary results on LED structures with optimized SEI layers confirm that the carrier overflow can indeed be eliminated while maintaining the active region quality. For optimum SEI layer design, which depends on the overall active region design, the resulting maximum EL efficiencies for single and quad 3 nm DH LEDs are similar. Further optimization of the SEI for various active regions designs is underway.

As observed in Fig. 2, the EL efficiency of hexa 3 nm DH LED is only slightly larger than that of the quad 3 nm DH, which suggests that the injected carriers are mostly consumed in the first four DH layers close to  $p$ -GaN due to limited hole transport for the achieved hole concentration and/or the active region quality may have slightly degraded with increased overall thickness. Further increase in the number of DH layers to 8 lowered the EL efficiency by  $\sim 20\%$  compared to the hexa 3 nm DH at a current density of  $350 \text{ A/cm}^2$ , which is a clear indication of the active layer quality degradation confirmed by PL measurements conducted at 10 K and 295 K (see Fig. 1).

It is worth noting that the EL efficiency for all the DH LEDs except the octa 3 nm DH show negligible drop with

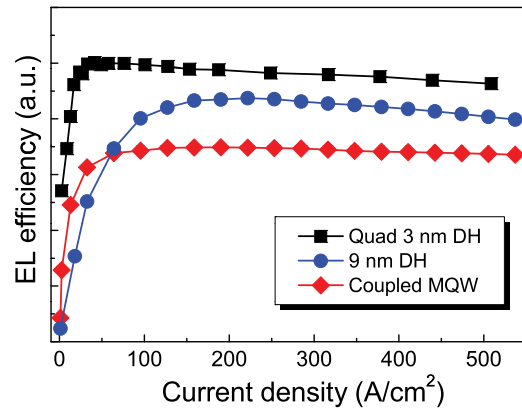


FIG. 3. EL efficiencies comparison for quad 3 nm DH, 9 nm DH, and coupled MQW (six period  $\text{In}_{0.15}\text{Ga}_{0.85}\text{N}$  (2 nm)/ $\text{In}_{0.06}\text{Ga}_{0.94}\text{N}$  (3 nm)) LEDs.

increasing injection current density up to  $500 \text{ A/cm}^2$ . PL and EL data in aggregate suggest that an active region with four DH layers (quad DH LED) provides an optimum design. In addition, as shown in Fig. 3, the quad 3 nm DH LED structure outperforms a typical MQW LED having the same total active layer thickness ( $6 \times 2 \text{ nm}$  well) and a DH LED with single 9 nm-thick active region, which was reported to have 1.25 and 3.8 times higher relative EL efficiency than 6 nm and 11 nm-thick single DH LEDs, respectively, at a current density of  $\sim 300 \text{ A/cm}^2$ .<sup>9</sup> Therefore, it is clear that multi-3 nm DH layer design is a superior approach for increasing the active region volume for enhanced light output and improvement of LED external quantum efficiency.

To conclude, multi-3 nm DH structures have been demonstrated to enhance the quantum efficiency of InGaN based LEDs at high injection levels. We showed that incorporating more DH layers (having 3D-like DOS) separated by thin and low InGaN barriers represents an effective avenue to improve light output compared with solely increasing single DH thickness or the number of 2 nm-thick QWs in MQW LEDs, which due to the two-dimensional DOS have limited optical output. Excitation dependent PL results indicate that PL efficiency is nearly proportional to the number of DH layers up to 6 at room temperature, suggesting the same quantum efficiency for each DH active layer. Similarly, EL efficiency is also shown to increase with the number of DH active layers up to 4, due to reduced electron leakage, and the hexa DH LED shows  $\sim 20\%$  higher EL efficiency than that of quad DH LED at high injection. We attribute the proportional increment in EL with increasing DH active region layers to increased carrier capture. Therefore, among the efforts to enhance the quantum efficiency at elevated injection levels, multi-DH layer designs with appropriate electron injectors can constitute a viable alternative approach to achieve high efficiency and high power LEDs.

The work at VCU is funded by a grant from the Air Force Office of Scientific Research. K.J. acknowledges support from BAFF.

<sup>1</sup>H. Morkoç, *Handbook of Nitride Semiconductors and Devices* (Wiley-VCH, 2008), Vol. 3, Chap. 1.

<sup>2</sup>B. Monemar and B. E. Sernelius, *Appl. Phys. Lett.* **91**, 181103 (2007).

<sup>3</sup>X. Li, X. Ni, J. Lee, M. Wu, Ü. Özgür, H. Morkoç, T. Paskova, G. Mulholland, and K. R. Evans, *Appl. Phys. Lett.* **95**, 121107 (2009).

- <sup>4</sup>B. J. Ahn, T. S. Kim, Y. Dong, M. T. Hong, J. H. Song, J.-H. Song, H. K. Yuh, S. C. Choi, D. K. Bae, and Y. Moon, *Appl. Phys. Lett.* **100**, 031905 (2012).
- <sup>5</sup>A. David, M. J. Grundmann, J. F. Kaeding, N. F. Gardner, T. G. Mihopoulos, and M. R. Krames, *Appl. Phys. Lett.* **92**, 053502 (2008).
- <sup>6</sup>J. P. Liu, J. H. Ryou, R. D. Dupuis, J. Han, G. D. Shen, and H. B. Wang, *Appl. Phys. Lett.* **93**, 021102 (2008).
- <sup>7</sup>N. F. Gardner, G. O. Müller, Y. C. Shen, G. Chen, S. Watanabe, W. Götz, and M. R. Krames, *Appl. Phys. Lett.* **91**, 243506 (2007).
- <sup>8</sup>M. Maier, T. Passow, M. Kunzer, W. Pletschen, K. Köhler, and J. Wagner, *Phys. Status Solidi C* **7**, 2148 (2010).
- <sup>9</sup>X. Li, S. Okur, F. Zhang, V. Avrutin, S. J. Liu, Ü. Özgür, H. Morkoç, S. M. Hong, S. H. Yen, T. S. Hsu, and A. Matulionis, *J. Appl. Phys.* **111**, 063112 (2012).
- <sup>10</sup>X. Li, F. Zhang, S. Okur, V. Avrutin, S. J. Liu, Ü. Özgür, H. Morkoç, S. M. Hong, S. H. Yen, T. S. Hsu, and A. Matulionis, *Phys. Status Solidi A* **208**, 2907 (2011).
- <sup>11</sup>J. Xie, Ü. Özgür, Y. Fu, X. Ni, H. Morkoç, C. K. Inoki, T. S. Kuan, J. V. Foreman, and H. O. Everitt, *Appl. Phys. Lett.* **90**, 041107 (2007).
- <sup>12</sup>S. Watanabe, N. Yamada, M. Nagashima, Y. Ueki, C. Sasaki, Y. Yamada, T. Taguchi, K. Tadamoto, H. Okagawa, and H. Kudo, *Appl. Phys. Lett.* **83**, 4906 (2003).
- <sup>13</sup>Y. J. Lee, C. H. Chiu, C. C. Ke, P. C. Lin, T. C. Lu, H. C. Kuo, and S. C. Wang, *IEEE J. Quantum Electron.* **15**, 1137 (2009).
- <sup>14</sup>J. Hader, J. V. Maloney, and S. W. Koch, *Appl. Phys. Lett.* **96**, 221106 (2010).
- <sup>15</sup>T. Malinauskas, A. Kadys, T. Grinys, S. Nargelas, R. Aleksiejunas, S. Miasojedovas, J. Mickevicius, R. Tomasiunas, K. Jarasiunas, M. Vengris, S. Okur, X. Li, F. Zhang, V. Avrutin, Ü. Özgür, and H. Morkoç, *Proc. SPIE* **8262**, 82621S (2012).
- <sup>16</sup>X. A. Cao, E. B. Stokes, P. M. Sandvik, S. F. LeBoeuf, J. Kretchmer, and D. Walker, *IEEE Electron Device Lett.* **23**, 535 (2002).
- <sup>17</sup>X. Ni, X. Li, J. Lee, S. Liu, V. Avrutin, Ü. Özgür, H. Morkoç, and A. Matulionis, *J. Appl. Phys.* **108**, 033112 (2010).